Exome sequencing identifies SLC17A9 pathogenic gene in two Chinese pedigrees with disseminated superficial actinic porokeratosis

Article *in* Journal of Medical Genetics · September 2014

DOI: 10.1136/jmedgenet-2014-102486 · Source: PubMed

CITATIONS
26

READS
73

26 authors, including:

Wenjun Wang
Cleveland State University
104 PUBLICATIONS **1,602** CITATIONS
SEE PROFILE

Zhen Yue
China National Genebank-Shenzhen
56 PUBLICATIONS **5,263** CITATIONS
SEE PROFILE

Xiaodong Zheng
346 PUBLICATIONS **8,105** CITATIONS
SEE PROFILE

Xianbo Zuo
Anhui Medical University
90 PUBLICATIONS **2,596** CITATIONS
SEE PROFILE

ORIGINAL ARTICLE

Exome sequencing identifies *SLC17A9* pathogenic gene in two Chinese pedigrees with disseminated superficial actinic porokeratosis

Hongzhou Cui,[1,2,3,4,5] Longnian Li,[1,4,5] Wenjun Wang,[1,4,5] Jie Shen,[1,4,5] Zhen Yue,[1,4,5] Xiaodong Zheng,[1,4,5] Xianbo Zuo,[1,4,5] Bo Liang,[1,4,5] Min Gao,[1,4,5] Xing Fan,[1,4,5] Xianyong Yin,[1,4,5] Changbing Shen,[1,4,5] Chao Yang,[1,4,5] Change Zhang,[1,4,5] Xiaoguang Zhang,[1,4,5] Yujun Sheng,[1,4,5] Jinping Gao,[1,4,5] Zhengwei Zhu,[1,4,5] Da Lin,[1,4,5] Anping Zhang,[1,4,5] Zaixing Wang,[1,4,5] Shengxiu Liu,[1,4,5] Liangdan Sun,[1,4,5] Sen Yang,[1,2,4,5] Yong Cui,[1,4,5] Xuejun Zhang[1,2,3,4,5]

▶ Additional material is published online only. To view please visit the journal online (http://dx.doi.org/10.1136/jmedgenet-2014-102486).

For numbered affiliations see end of article.

Correspondence to
Yong Cui, Institute of Dermatology and Department of Dermatology at No. 1 Hospital, Anhui Medical University, Hefei, Anhui 230032, China;
wuhucuiyong@vip.163.com

HZC and LNL contributed equally.

Received 22 April 2014
Revised 6 August 2014
Accepted 7 August 2014

ABSTRACT

Background Disseminated superficial actinic porokeratosis (DSAP) is a rare autosomal dominant genodermatosis characterised by annular lesions that has an atrophic centre and a prominent peripheral ridge distributed on sun exposed area. It exhibits high heterogeneity, and five linkage loci have been reported. The mevalonate kinase (*MVK*) gene located on 12q24 has been confirmed as one of the disease-causing genes. But, the pathogenesis of a large part of DSAP remains unclear so far.

Methods The recruited with DSAP carried no *MVK* coding mutations. Exome sequencing was performed in two affected and one unaffected individual in Family 1. Cosegregation of the candidate variants was tested in other family members. Sanger sequencing in 33 individuals with familial DSAP and 19 sporadic DSAP individuals was performed for validating the causative gene.

Results An average of 1.35×10^5 variants were generated from exome data and 133 novel NS/SS/indels were identified as being shared by two affected individuals but absent in the unaffected individual. After functional prediction, 25 possible deleterious variants were identified. In Family 1, a missense variant c.932G>A (p.Arg311Gln) in exon 10 of *SLC17A9* was observed in cosegregation with the phenotype; this amino acid substitution was located in a highly conserved major facilitator superfamily (MFS) domain in multiple mammalian. One additional missense variant c.25C>T (p.Arg9Cys) in exon 2 of *SLC17A9* was found in Family 2.

Conclusions The result identified *SLC17A9* as another pathogenic gene for DSAP, which suggests a correlation between the aberrant vesicular nucleotide transporter and the pathogenesis of DSAP.

To cite: Cui H, Li L, Wang W, *et al*. *J Med Genet* Published Online First: [*please include* Day Month Year] doi:10.1136/jmedgenet-2014-102486

INTRODUCTION

Porokeratosis is a group of rare keratinisation disorders with characteristic cornoid lamella in pathology. Cornoid lamella forms from keratin columns and is clinically characterised by one or more annular lesions with an atrophic fovea and raised horny border which spread centrifugally. Historically, porokeratosis was classified into the following five subtypes based on clinical features: porokeratosis of Mibelli, disseminated superficial porokeratosis, disseminated superficial actinic porokeratosis (DSAP), porokeratosis palmaris et plantaris disseminated, liner porokeratosis. DSAP is the most common porokeratosis subtype and manifests as multiple, small, annular, anhidrotic, keratotic lesions and mainly distributes on the sun exposed area. DSAP is transmitted as the autosomal dominant trait. To date, five linkage loci for DSAP reported previously support its heterogeneity (12q23.2–24.1,[1] 12q24.1–q24.2,[2] 15q25.1–26.1,[3] 1p31.3–p31.1[4] and 16q24.1–24.3[5]). *SART3* and *SSH1* genes had been identified responsible for different DSAP families.[2 6] In 2012, our team performed whole-exome sequencing in a Chinese DSAP family. The result reveals that the heterozygous substitution variant c.764T>C (p.Leu255Pro) in the mevalonate kinase (*MVK*) gene serves as the disease-causing gene. Overall, 13 different *MVK* coding variants were discovered in 18 additional DSAP families and four sporadic cases.[7] The identification of *MVK coding* variants in other studies further supports the role of *MVK* as a pathogenic gene in DSAP. However, DSAP is a heterogeneous disease and a large portion of the recruited patients with DSAP did not carry the *MVK* variant.

In this study, we performed exome sequencing and mutational analyses in DSAP patients without *MVK*, *SART3* and *SSH1* exons and splice-site variants and identified the pathogenic role of two *SLC17A9* variants in two DSAP families.

MATERIALS AND METHODS

Seven families (Families 1–7) and 19 sporadic DSAP patients without *MVK*, *SART3* and *SSH1* coding variants were recruited from the Institute of Dermatology, Anhui Medical University, China. All the patients were provided correct diagnoses by experienced dermatologists. The individuals participating from Families 1 to 7 included 21 affected and 12 unaffected individuals (figures 1 and 2, see online supplementary figure S1). Moreover, we

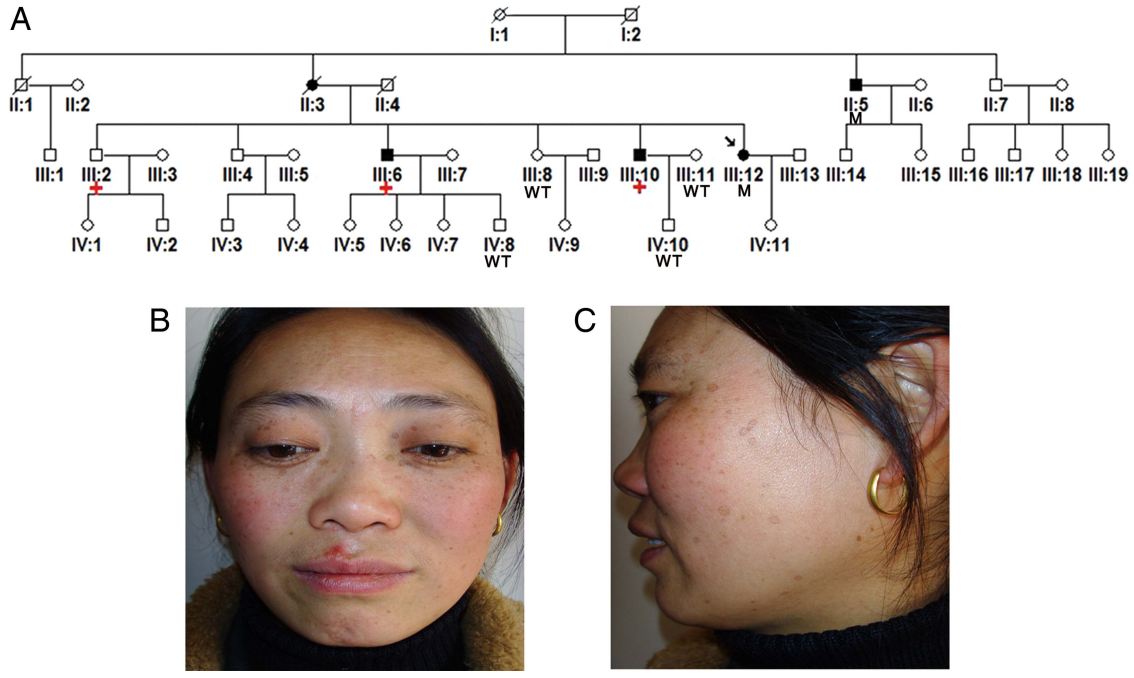

Figure 1 The genealogical trees and clinical manifestations of the proband in Family 1. (A) The genealogical tree of Family 1. '+' indicates the individuals subject to exome sequencing, 'WT' indicates the wildtype carriers in *SLC17A9* sequence analysis and 'M' indicates mutated *SLC17A9* individuals who were sequenced in this study. (B and C) The clinical features of the proband in Family 1. The proband III:12 is a 39-year-old woman who began to develop several tiny papules on the face at 20 years of age. The papules spread centrifugally and grew increasingly. The typical annual keratin lesions are mainly distributed on the forehead, cheek and around the eyes.

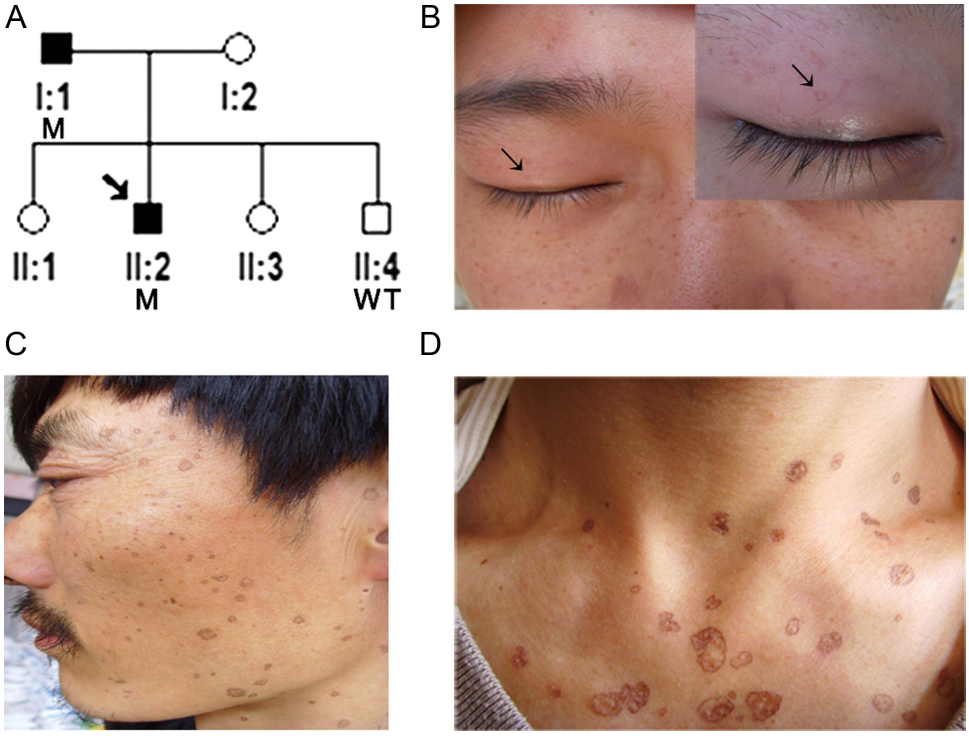

Figure 2 The pedigree and clinical manifestations of the affected individuals in Family 2. (A) The genealogical tree of Family 2. 'WT' and 'M' indicate individuals carrying wildtype and mutated *SLC17A9* coding sequence. (B–D) The clinical characteristics of the patients in Family 2. The proband (II:2) is a 19-year-old man. Upon examination, numerous tiny papules distributed on the face were observed, and the black arrows indicate an annular lesion with atrophic fovea and raised horny borders in the eyelids. The father (I:1), a 46-year-old man, displayed numerous bean-size brown keratotic plaques distributed on the face, chest and forearms.

have exome sequencing data of 676 unrelated normal Chinese populations and 781 unrelated, ethnically and geographically matched patients of other diseases to exclude possible polymorphisms and systematic artefacts. After informed consent, genomic DNAs were extracted from blood samples using the Qiagen blood kits. This study was authorised by the ethics committee of Anhui Medical University and all work was done in accordance with Helsinki principles.

Exome capture and sequencing

The purified DNA samples were randomly fragmented into 150–200 bp lengths. The fragments were ligated with adapter and amplified by ligation-mediated PCR. PCR product enrichment was carried out to obtain the exon-enriched hybridised fragments using the Agilent SureSelect Human All Exon Kit (Qiagen, California, USA). Each captured library was then loaded on a HiSeq 2000 platform (Illumina, San Diego, California, USA). Raw image file was recognised by Illumina basecalling 1.7 software (Illumina) and 90 bp pair-end reads were obtained. We used SOAPaligner (SOAP 2.21) to map reads onto the reference genome (National Center for Biotechnology Information (NCBI) build 37.3, hg19) for detecting variants. SOAPsnp (V.1.03) (BGI, Shenzhen, China) and genome analysis toolkit (Broad Institute, Harvard University, USA) software were used for calling SNP variants and insertion/deletion (indel) variants, respectively.

Functional annotation of genetic variants

Common variants were eliminated when identified in Single Nucleotide Polymorphism Database (dbSNP135), the 1000 Genome Project, eight HapMaps and inhouse database. We obtained variants that were shared between two cases and absent in the control.

We first chose the variants located in the linkage intervals and detected the candidate variants in other pedigree members. If no variant was located inside the linkage intervals or the candidate variants were not validated, functional predictions using Sorting Intolerant From Tolerant (SIFT, http://sift.jcvi.org) and Polymorphism Phenotyping (Polyphen, http://genetics.bwh.harvard.edu/pph/) programs were performed for an extended range of variants throughout the entire exome. Potentially functional variants were selected for Sanger sequencing. The causative variants should comply with cosegregation between the genotypes and phenotypes.

Sanger sequencing and mutation analysis

All of the primes cover all the exons, and intron–exon boundaries of *SLC17A9* gene were designed using the Primer Premier 5.0 program (Premier Biosoft, Palo Alto, California, USA). PCR amplification performed in an ABI 9700 Thermal Cycler (Applied Biosystems, Carlsbad, California, USA). The products were purified using a QIAquick PCR Purification Kit (Qiagen) and sequenced using an ABI PRISM 3730 automated sequencer (Applied Biosystems). Chromas (V.3.0) was used to read the amplification fragment.

RESULTS

Clinical features

Seven families (Families 1–7) and 19 sporadic patients with DSAP were selected based on characteristic irregular annular keratotic lesions with slightly elevated borders. The mean onset age was 18.2 years and ranged from 13 to 32 years. None of the patients were affected with carcinoma. Sanger sequencing revealed that none of the patients carried *MVK, SART3* and *SSH1* coding variants. We selected two affected individuals (III:6, III:10) and one unaffected individual (III:2) from Family 1 for exome sequencing. The proband (III:12) was a 39-year-old woman who experienced onset at the age of 20. Tiny papules initially appeared on face. These papules gradually spread centrifugally and grew to involve the cheek, forehead and area around the eyes (figure 1).

Exome sequencing identifies *SLC17A9* variant in Family 1

After exome capturing, an average of 5.18 Gb of paired-end, 90-bp length reads per individual were obtained. We mapped the sequence data to the human reference genome (NCBI Build 37, hg19), discarded the reads with duplicated start sites and achieved a 3.40 Gb targeted exome with 67-fold depth defined by RefSeq genes. On average, 87% of the exomes were covered at least 10-fold (see online supplementary table S1). By annotating variants, we primarily focus on potentially functional variants including non-synonymous variants, splice-site variants and insertions/deletions (indels) absent in dbSNP135, 8 HapMaps, the 1000 Genomes Project and 1457 unrelated exome data. In all, 133 variants were selected and four of these variants were located within the loci that have been linked to DSAP in previous linkage studies (table 1). Sanger sequencing failed to confirm the disease gene because we did not observe cosegregation with the phenotypes in the family.

Table 1 The screening process in identifying the potential variants from exome data

	Family 1- III:2	Family 1- III:6	Family 1- III:10
Total SNPs and indels	40 782 and 2564	46 205 and 2729	51 685 and 2080
Potential SNPs and indels*	10 704 and 572	10 834 and 619	10 166 and 688
Filtered_dbSNP	1187 and 154	1215 and 148	1642 and 194
Filtered_dbSNP_1000genomes	613 and 56	720 and 45	887 and 67
Filtered_dbSNP_1000genomes_Hapmap8	575 and 50	680 and 40	796 and 53
Filtered_dbSNP_1000genomes_Hapmap8_1457 exome	358 and 27	428 and 19	464 and 24
Filtered_dbSNP_1000genomes_Hapmap8_1457 exome_Family 1-III:2	0	128 and 5	
Within the linkage region†	Four genes (*C12orf42, RIC8B, C1orf173* and *CTU2*)		
Functional prediction by SIFT and Polyphen-2	nineteen SNPs (non-benign and non-tolerant) and six indels		
Mutation analysis	c.932G>A (p.Arg311Gln) in exon 10 of *SLC17A9*		

*Potential SNP and indels include non-synonymous variants, splicing site variants and insertion/deletion variants located in exonic region.
†The linkage regions refer to chromosomes 12q23.2–24.1, 12q24.1–q24.2, 15q25.1–26.1, 1p31.3–p31.1 and 16q24.1–24.3 reported previously.
Polyphen, Polymorphism Phenotyping; SIFT, Sorting Intolerant From Tolerant; SNP, single nucleotide polymorphism; dbSNP, Single Nucleotide Polymorphism Database.

Expanding to the whole exome, SIFT and Polyphen were used to predict whether a variant is damaging. In total, 25 suspected functional variants were obtained and sent for Sanger sequencing (see online supplementary table S2). Among these variants, we observed a cosegregation of one missense variant c.932G>A (p.Arg311Gln) in *SLC17A9* with the phenotype in Family 1 (table 1). This variant lies in exon 10 of *SLC17A9* and replaces a highly conserved arginine residue with glutamine at position 311. The amino acid residue is located in the major facilitator superfamily (MFS) domain, general substrate transporter (MFS_dom_general_subst_transpt) (figure 3). This variant was not detected in 1457 unrelated individuals.

Mutational analyses in *SLC17A9* gene

To confirm the pathogenic *SLC17A9* gene, all 15 exons and intron–exon boundaries of *SLC17A9* gene were sequenced in the other six families (Families 2–7) and 19 sporadic patients (see online supplementary table S3). One additional missense variant c.25C>T (p.Arg9Cys) in exon 2 of *SLC17A9* was identified in Family 2; this variant led an amino acid substitution from arginine to cysteine, which was also located in MFS_dom_general_subst_transpt (figure 3). It was not identified in 1457 unrelated individuals. The results suggest that *SLC17A9* is a causative gene for DSAP.

DISCUSSION

DSAP is a heterogeneous disease. Previous studies had revealed five loci and a few disease genes in DSAP, but the causative agent remains unclear for many patients with DSAP. Here, we performed exome sequencing and mutational analyses in the families lacking *MVK* coding variants and identified two *SLC17A9* gene variants in DSAP.

The *SLC17A9* gene is located on chromosome 20q13.33 and spanned 15 exons. The encoded protein is a vesicular nucleotide transporter (VNUT) that contains 436 aa residues. Sawada and colleagues first identified this protein as a coiled 12 transmembrane domains across the membranes with the NH2-terminal and COOH-terminal tails facing the cytosol. VNUT orthologues are widely distributed in the vertebrates and invertebrates.[8] In humans, SLC17A9 was widely expressed in various organs and was also expressed in epidermal keratinocytes, and the expression of VNUT may be a target of anti-inflammatory response in skin cells.[9]

The VNUT, coded by *SLC17A9*, contributed to ATP vesicle formation and regulated ATP release. Two pathways had been found to govern cellular ATP release: transporter/channel-mediated release and the exocytosis of ATP-containing vesicles. During vesicle fusion with the plasma membrane, vesicle-bound ATP transporters are incorporated into the membrane and contribute to ATP efflux. Studies have demonstrated the vital role of loading ATP from the cytoplasm into vesicles in vesicle

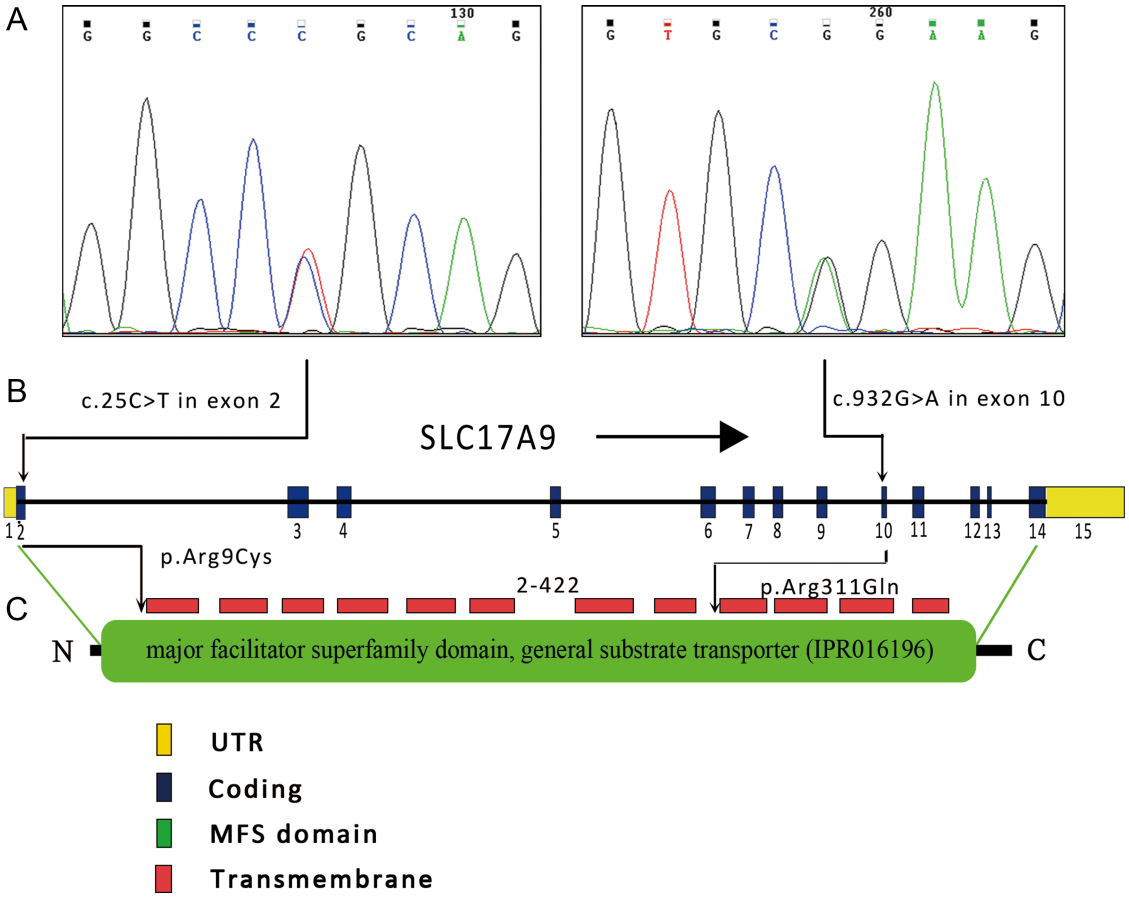

Figure 3 The mutation analysis, exon and intron organisation and domain structure of *SLC17A9*. (A) c.25C>T in Family 2 and c.932G>A in Family 1. (B) The positions of the missense mutation c.932G>A in exon 10 and c.25C>T in exon 2 of *SLC17A9* are indicated by black fold arrows. The yellow and dark-blue shaded boxes represent UTR exons and coded exons, respectively. (C) The positions of amino acid residue substitutions of p.Arg9Cys and p.Arg311Gln are indicated by black fold arrows. The green and red shaded box represents the predicted functional domain and transmembrane regions. UTR, untranslated region; MFS, major facilitator superfamily.

formation.[10 11] In addition to the collaborative pathways, VNUT-dependent pathways can contribute separately to the release of ATP.[12]

ATP efflux can serve as a local signalling to facilitate cytosolic Ca^{2+} release.[13] Extracellular ATP is activated in the iron channels and facilitates the release of effective factors.[14] In keratinocytes, extracellular calcium concentrations can significantly affect proliferation and differentiation. By increasing extracellular calcium concentration, a series of effector proteins, such as desmoplakin, cadherins, integrins, catenins, plakoglobulin and keratins, are redistributed from the cytosol to the membrane. Some differentiation-specific proteins were also elevated.[15] Additional evidence indicates that increased proliferation is caused by increased intracellular calcium concentrations or loss of the calcium gradient.[16–18]

In this study, the identified 9th and 311th amino acid residues were located on MFS domain, general substrate transporter (figure 3). This member of MFS was previously found in lycerol-3-phosphate transporter which acted on transport glycerol-3-phosphate into the cytoplasm and inorganic phosphate into the periplasm. It was also found in proton/sugar transporter lactose permease with a function to couple lactose and H^+ translocation in *Escherichia coli*.[19 20] The 9th residues were 15 amino acids away from the first transmembrane helical structure and the 311th had two amino acids distance to the nine transmembrane helix (see online supplementary figure S2). The substitution of these residues altered polarity and charge of amino acids and subsequently affected protein structure stability and property of membrane fusion. In addition, the suspected residues were located in a side opening near the mouth of the channel constructed by transmembrane domains. This type of residue exerts an electrical charge that permits or repels ion streams, especially for calcium concentrations.[21] Defective VNUT can delay the ATP efflux and calcium release into periplasm. G-protein-coupled receptor serves as one target receptor to sense the change in calcium and implicates in activating a series of pathways, like protein kinase C pathway, which results in increased proliferation.

In conclusion, DSAP is a keratinisation disorder with unique parakeratotic and hyperkeratotic cornoid lamella. We demonstrate a pathogenic role for *SLC17A9* in two DSAP families. The probable mechanism may be associated with abnormal ion influx/efflux of transmembrane Ca^{2+} and accompanying ATP release. Further studies are needed to confirm the causative gene in more patients with DSAP and uncover the functional mechanisms.

Author affiliations
[1]Institute of Dermatology and Department of Dermatology at No.1 Hospital, Anhui Medical University, Hefei, Anhui, China
[2]Department of Dermatology, Huashan Hospital of Fudan University, Shanghai, China
[3]Department of Dermatology at No.2 Hospital, Anhui Medical University, Hefei, Anhui, China
[4]Department of Dermatology and Venereology, Anhui Medical University, Hefei, Anhui, China
[5]State Key Laboratory Incubation Base of Dermatology, Ministry of National Science and Technology & Key Laboratory of Dermatology, Ministry of Education & Key Laboratory of Dermatology, Hefei, Anhui, China

Acknowledgements We are grateful to the participants involved in this study. This project was funded by Ministry of Education of China (IRT-1046), National Natural Science Foundation of China (Grant No. 31171223), Program for New Century Excellent Talents in University (NCET-12-0600), Program for Changjiang Scholars and Innovative Research Team in University and Program for Outstanding Talents of Anhui Medical University.

Contributors DL, AZ, ZW and SL recruited samples. BL and CS reserved and prepared the blood samples. WW, CY, ZZ, JS and ZY conducted DNA extraction. YS and MG undertook the exome capture. XF and XBZ analysed the whole-exome sequencing data. XDZ performed variants filtering. JG and CZ participated in Sanger sequencing. XY and XGZ read the variants. YC provided 1457 exome data. HC and LL wrote and revised the manuscript. YC, XJZ, SY and LS designed the project.

Competing interests None.

Patient consent Obtained.

Ethics approval The Ethics Committee of the Anhui Medical University.

Provenance and peer review Not commissioned; externally peer reviewed.

REFERENCES

1 Xia JH, Yang YF, Deng H, Tang BS, Tang DS, He YG, Xia K, Chen SX, Li YX, Pan Q, Long ZG, Dai HP, Liao XD, Xiao JF, Liu ZR, Lu CY, Yu KP, Deng HX. Identification of a locus for disseminated superficial actinic porokeratosis at chromosome 12q23.2-24.1. *J Invest Dermatol* 2000;114:1071–4.
2 Zhang ZH, Niu ZM, Yuan WT, Zhao JJ, Jiang FX, Zhang J, Chai B, Cui F, Chen W, Lian CH, Xiang LH, Xu SJ, Liu WD, Zheng ZZ, Huang W. A mutation in SART3 gene in a Chinese pedigree with disseminated superficial actinic porokeratosis. *Br J Dermatol* 2005;152:658–63.
3 Xia K, Deng H, Xia JH, Zheng D, Zhang HL, Lu CY, Li CQ, Pan Q, Dai HP, Yang YF, Long ZG, Deng HX. A novel locus (DSAP2) for disseminated superficial actinic porokeratosis maps to chromosome 15q25.1-26.1. *Br J Dermatol* 2002;147:650–4.
4 Liu P, Zhang S, Yao Q, Liu X, Wang X, Huang C, Huang X, Wang P, Yuan M, Liu JY, Wang QK, Liu M. Identification of a genetic locus for autosomal dominant disseminated superficial actinic porokeratosis on chromosome 1p31.3-p31.1. *Hum Genet* 2008;123:507–13.
5 Luan J, Niu Z, Zhang J, Crosby ME, Zhang Z, Chu X, Wang Z, Huang W, Xiang L, Zheng Z. A novel locus for disseminated superficial actinic porokeratosis maps to chromosome 16q24.1-24.3. *Hum Genet* 2011;129:329–34.
6 Zhang Z, Niu Z, Yuan W, Liu W, Xiang L, Zhang J, Chu X, Zhao J, Jiang F, Chai B, Cui F, Wang Y, Zhang K, Xu S, Xia L, Gu J, Zhang S, Meng X, Wang S, Gao S, Fan M, Nie L, Zheng Z, Huang W. Fine mapping and identification of a candidate gene SSH1 in disseminated superficial actinic porokeratosis. *Hum Mutat* 2004;24:438.
7 Zhang SQ, Jiang T, Li M, Zhang X, Ren YQ, Wei SC, Sun LD, Cheng H, Li Y, Yin XY, Hu ZM, Wang ZY, Liu Y, Guo BR, Tang HY, Tang XF, Ding YT, Wang JB, Li P, Wu BY, Wang W, Yuan XF, Hou JS, Ha WW, Wang WJ, Zhai YJ, Wang J, Qian FF, Zhou FS, Chen G, Zuo XB, Zheng XD, Sheng YJ, Gao JP, Liang B, Zhu J, Xiao FL, Wang PG, Cui Y, Li H, Liu SX, Gao M, Fan X, Shen SK, Zeng M, Sun GQ, Xu Y, Hu JC, He TT, Li YR, Yang HM, Yu ZY, Zhang HF, Hu X, Yang K, Zhao SX, Zhou YW, Liu JJ, Du WD, Zhang L, Xia K, Yang S, Zhang XJ. Exome sequencing identifies MVK mutations in disseminated superficial actinic porokeratosis. *Nat Genet* 2012;44:1156–60.
8 Sawada K, Echigo N, Juge N, Miyaji T, Otsuka M, Omote H, Yamamoto A, Moriyama Y. Identification of a vesicular nucleotide transporter. *Proc Natl Acad Sci USA* 2008;105:5683–6.
9 Inoue K, Komatsu R, Imura Y, Fujishita K, Shibata K, Moriyama Y, Koizumi S. Mechanism underlying ATP release in human epidermal keratinocytes. *J Invest Dermatol* 2014;134:1465–8.
10 Sathe MN, Woo K, Kresge C, Bugde A, Luby-Phelps K, Lewis MA, Feranchak AP. Regulation of purinergic signaling in biliary epithelial cells by exocytosis of SLC17A9-dependent ATP-enriched vesicles. *J Biol Chem* 2011;286:25363–76.
11 Sesma JI, Esther CR Jr, Kreda SM, Jones L, O'Neal W, Nishihara S, Nicholas RA, Lazarowski ER. Endoplasmic reticulum/golgi nucleotide sugar transporters contribute to the cellular release of UDP-sugar signaling molecules. *J Biol Chem* 2009;284:12572–83.
12 Sesma JI, Kreda SM, Okada SF, van Heusden C, Moussa L, Jones LC, O'Neal WK, Togawa N, Hiasa M, Moriyama Y, Lazarowski ER. Vesicular nucleotide transporter regulates the nucleotide content in airway epithelial mucin granules. *Am J Physiol Cell Physiol* 2013;304:C976–84.
13 Arcuino G, Lin JH, Takano T, Liu C, Jiang L, Gao Q, Kang J, Nedergaard M. Intercellular calcium signaling mediated by point-source burst release of ATP. *Proc Natl Acad Sci USA* 2002;99:9840–5.
14 Tokunaga A, Tsukimoto M, Harada H, Moriyama Y, Kojima S. Involvement of SLC17A9-dependent vesicular exocytosis in the mechanism of ATP release during T cell activation. *J Biol Chem* 2010;285:17406–16.
15 Gibson DF, Ratnam AV, Bikle DD. Evidence for separate control mechanisms at the message, protein, and enzyme activation levels for transglutaminase during calcium-induced differentiation of normal and transformed human keratinocytes. *J Invest Dermatol* 1996;106:154–61.
16 Lee SH, Elias PM, Proksch E, Menon GK, Mao-Quiang M, Feingold KR. Calcium and potassium are important regulators of barrier homeostasis in murine epidermis. *J Clin Invest* 1992;89:530–8.

17 Menon GK, Elias PM, Lee SH, Feingold KR. Localization of calcium in murine epidermis following disruption and repair of the permeability barrier. *Cell Tissue Res* 1992;270:503–12.
18 Mauro T, Bench G, Sidderas-Haddad E, Feingold K, Elias P, Cullander C. Acute barrier perturbation abolishes the Ca2+ and K+ gradients in murine epidermis: quantitative measurement using PIXE. *J Invest Dermatol* 1998;111:1198–201.
19 Huang Y, Lemieux MJ, Song J, Auer M, Wang DN. Structure and mechanism of the glycerol-3-phosphate transporter from Escherichia coli. *Science* 2003;301:616–20.
20 Mirza O, Guan L, Verner G, Iwata S, Kaback HR. Structural evidence for induced fit and a mechanism for sugar/H+ symport in LacY. *EMBO J* 2006;25:1177–83.
21 Reyes N, Gadsby DC. Ion permeation through the Na+,K+-ATPase. *Nature* 2006;443:470–4.